



30th Eurosensors Conference, EUROSENSORS 2016

Embedded control of a PMSM servo drive without current measurements

Dino Hüllmann*, Harald Kohlhoff, Patrick Neumann

Bundesanstalt für Materialforschung und -prüfung, Unter den Eichen 87, 12205 Berlin, Germany

Abstract

A permanent-magnet synchronous motor (PMSM) servo drive for lightweight robotic platforms that have a high torque demand at low rotational speeds has been developed. First, a current-independent torque controller is derived and cascaded with a speed and position controller, while merely an encoder is used as a sensor device in combination with a speed estimator. Finally, the speed estimator output is compared to gyroscope measurements and the overall functioning is verified on a real system.

© 2016 The Authors. Published by Elsevier Ltd. This is an open access article under the CC BY-NC-ND license

(<http://creativecommons.org/licenses/by-nc-nd/4.0/>).

Peer-review under responsibility of the organizing committee of the 30th Eurosensors Conference

Keywords: PMSM ; BLDC ; servo drive ; control ; optical incremental encoder ; speed estimator

1. Introduction

The permanent-magnet synchronous motor (PMSM) combines several advantages compared to classical motor types: high power and torque density, efficiency, reliability, low inertia and high dynamics. Even though this comes at the cost of a more complex control scheme, these characteristics make the PMSM well-suited for applications where size and weight matter, e.g. mobile robotics. Particularly, servo drives used as actuators can benefit from it.

Modern sensorless algorithms estimate speed and position by means of current measurements, but they aim at high-speed drives and cannot be applied to comparatively slow servo applications [1]. Hence, additional sensors are used to measure position and speed, while current measurements are still required. In this paper, an approach is

* Corresponding author. Tel.: +49-30-8104-4790; fax: +49-30-8104-1917.

E-mail address: dino.huellmann@bam.de

presented that does not depend on current measurements and, instead, derives all quantities from an optical incremental encoder.

2. Mathematical model of the PMSM

Initially, a mathematical model of the PMSM is needed to design a suitable controller. The underlying equations describing the system dynamics can be found in [2] or virtually all papers about field-oriented or vector control (FOC).

The stator voltage can be expressed in the stator reference frame S , usually called the $\alpha\beta$ reference frame [3], as

$$\mathbf{u}^S = R_S \cdot \mathbf{i}^S + \frac{d}{dt} \Psi^S = R_S \cdot \mathbf{i}^S + \frac{d}{dt} (L_S \cdot \mathbf{i}^S + \Psi_m^S) \quad (1)$$

with R_S being the resistance of the stator windings and \mathbf{i}^S being the 3-phase currents. Ψ_S is the stator flux, L_S describes the self-inductance of the stator and Ψ_m^S is the contribution of the rotor flux. The latter can be treated as a constant in the rotor reference frame R , i.e. $\Psi_m^R = \psi_{PM}$. Usually, this frame is named dq coordinate system [3] and can be simply transformed into the stator system S by rotating it through the electrical rotor angle ϑ :

$$\Psi_m^S = e^{j\vartheta} \cdot \Psi_m^R = e^{j\vartheta} \cdot \psi_{PM} \quad \text{with } j^2 = -1 \quad (2)$$

The essential control parameter, however, is the torque generated by the motor, which is given by

$$\tau_M = \frac{3}{2} \cdot p \cdot \psi_{PM} \cdot \text{Im}[\mathbf{i}^R] = \frac{3}{2} \cdot p \cdot \psi_{PM} \cdot \text{Im}[e^{-j\vartheta} \cdot \mathbf{i}^S] \quad (3)$$

with p being the number of pole pairs of the motor. This number also gives a relation between the electrical and the mechanical rotor angle: $= p \cdot \vartheta_{\text{mech}}$. At this point, a usual field-oriented controller would come into operation, trying to adjust \mathbf{i}^S so that the desired torque is delivered. Instead, we insert (2) and (3) into (1):

$$\mathbf{u}^S = R_S \cdot \mathbf{i}^S + L_S \frac{d}{dt} \mathbf{i}^S + j \cdot e^{j\vartheta} \cdot \dot{\vartheta} \cdot \psi_{PM} \quad (4)$$

Let the applied stator voltages be $\mathbf{u}^S = e^{j\varphi} \cdot \hat{\mathbf{u}}$, with φ being the commanded angle of the electrical field. Further, $\mathbf{i}^S = e^{j\gamma} \cdot \hat{\mathbf{i}}$ may denote the currents caused by these voltages. In general, the currents are out-of-phase with the voltages and therefore the angle γ differs from φ . Inserting these definitions into (4) yields

$$e^{j(\varphi-\vartheta)} \cdot \hat{\mathbf{u}} = (R_S + j L_S \dot{\gamma}) e^{j\gamma} \cdot e^{-j\vartheta} \cdot \hat{\mathbf{i}} + j \dot{\vartheta} \psi_{PM} \quad (5)$$

$$\mathbf{i}^S = e^{j\gamma} \cdot \hat{\mathbf{i}} = e^{j\vartheta} \frac{e^{j(\varphi-\vartheta)} \cdot \hat{\mathbf{u}} - j \dot{\vartheta} \psi_{PM}}{R_S + j L_S \dot{\gamma}} \quad (6)$$

Typically, servo PMSM are characterized by specific parameter ratios: $R_S = 14.4 \Omega$ and $L_S = 2 \text{ mH}$ are exemplary values for a small motor with stator dimension $8 \times \emptyset 22 \text{ mm}$, 7 pole pairs and 80 windings. In case of servo motors these parameters are optimized for high torque and not for high speed operation.

Assuming the maximum rotational speed of the motor is $\dot{\vartheta}_{\text{max}} = 240 \text{ rpm} = 8\pi \text{ rad/s}$, the maximum rate of change of the current angle γ becomes $\dot{\gamma}_{\text{max}} = p \cdot \dot{\vartheta}_{\text{max}} = 56\pi \text{ rad/s}$, if short time switching effects are neglected. Thus, $R_S = 14.4 \Omega \gg L_S \cdot \dot{\gamma} = 0.35 \Omega$ holds and the imaginary part of the denominator in (6) might be neglected:

$$\tau_M = \frac{3}{2} \cdot \frac{p \cdot \psi_{PM}}{R_S} (\hat{\mathbf{u}} \cdot \sin(\varphi - \vartheta) - \psi_{PM} \cdot \dot{\vartheta}) \quad (7)$$

The sinus term conforms to the well-known property of synchronous machines to generate most torque if the electrical field is 90° ahead or behind the electrical rotor position.

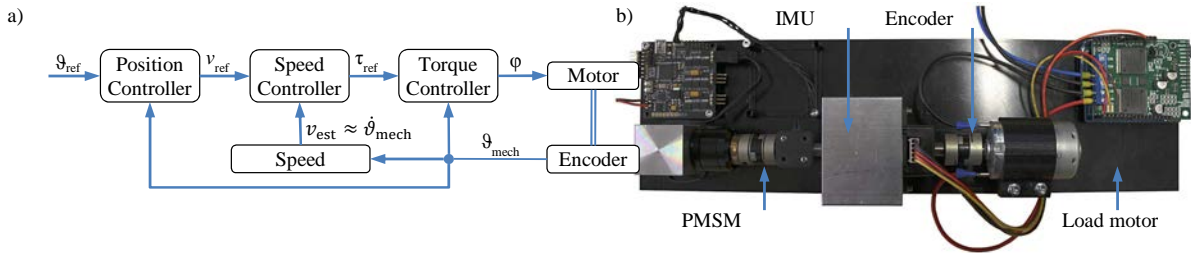


Fig. 1. a) Control structure, b) The motor test bed setup used in the experiments.

3. Control structure of the servo drive

Servo drives often consist of a torque, speed and position controller. This proven concept is also applied in this work, as shown in fig. 1a. Optical incremental encoders do not provide a speed signal themselves, therefore the setup is augmented with an additional speed estimator, which is described in the next section.

Since friction can only decrease the acting torque and the cascaded controller is able to compensate deviations at the torque level, we may neglect all friction terms. Moreover, we assume a constant voltage supply \hat{u} and do a first-order Taylor approximation of the sine term in (7) around the point $\varphi - \vartheta = 0$. Inserting these approximations yields

$$\tau_M = C_1 \cdot (\varphi - \vartheta) = C_1 \cdot (\varphi - p \cdot \vartheta_{mech}) \tag{8}$$

with $C_1 = 3/2 \cdot p \cdot \psi_{PM} / R_S \cdot \hat{u} = \text{const.}$ By solving (8) for the control input φ , that is the predefined angle of the electrical field, we obtain the underlying equation of the torque controller:

$$\varphi(t) = \frac{\tau_{ref}(t)}{C_1} + p \cdot \vartheta_{mech}(t) \tag{9}$$

Since the rate of change of speed, $\dot{\vartheta}_{mech}$, is directly proportional to the applied torque, a proportional-integral controller (PI controller) is chosen to adjust the rotational velocity and to overcome steady-state errors caused by friction and other neglected or unpredictable effects. In contrast, a simple P-controller is chosen for the positional part.

4. Speed estimation

In [4] different velocity estimation approaches using incremental encoders are compared. One method promises very low relative errors while having modest system requirements. Basically, a timestamp is assigned to each detected encoder tick. Now, let $n(t)$ denote the encoder tick count at time t , then the velocity can be estimated as

$$v_{est}(t) = \frac{n(t_2) - n(t_1)}{t_2 - t_1} \quad t_2 > t_1 \tag{10}$$

with t_2 being the most recent timestamp at time t and a minimal time interval between t_1 and t_2 , i.e. $t_2 - t_1 \geq \Delta t_{min}$.

5. Experimental results

To test the performance of the proposed servo controller, a motor test bed was built. Its main components are the PMSM with the specifications given above as well as an optical incremental encoder and an inertial measurement unit (IMU) that are connected to the motor shaft (see fig. 1b). Firstly, the output of the speed estimator has to be verified. For this purpose, trajectories are generated by turning the motor by hand, as the example in fig. 2 shows. From the plot on the right side it can be seen that there is a systematic error portion between both signals. However, in all recorded tests the root-mean-square error was smaller than $0.2 \text{ rad/s} < 2 \text{ rpm}$. This is sufficient for our purpose.

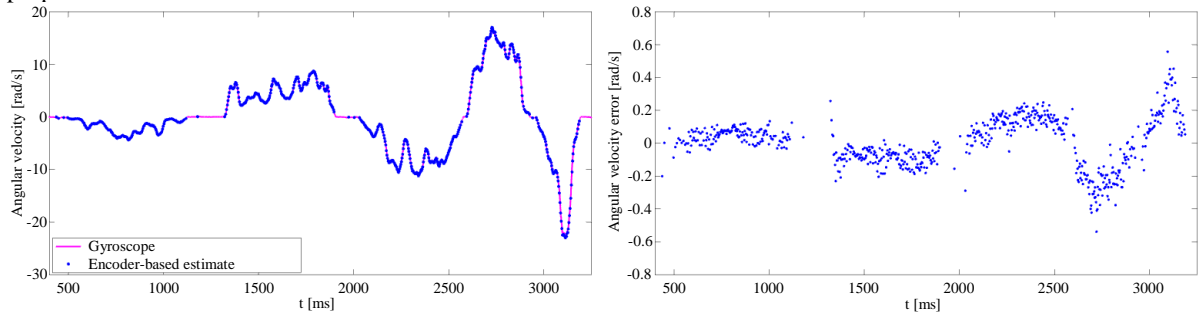


Fig. 2. Angular velocity measured with a gyroscope compared to the estimator using encoder measurements, $\Delta t_{\min} = 3 \text{ ms}$.

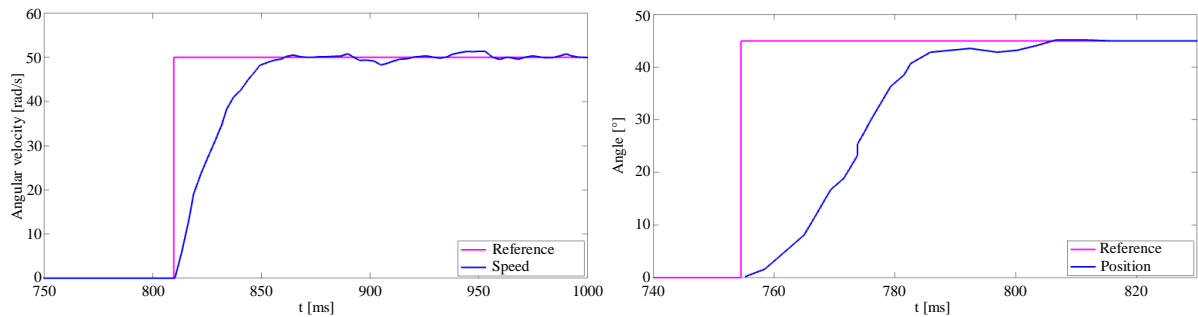


Fig. 3. Step response of the speed controller (left) and the position controller (right).

In fig. 3, a step response of the speed and the position controller are shown. Both controllers were only slightly tuned, so probably a better performance could be achieved using more suitable parameters. However, as the speed step response shows, the angular velocity fluctuates around the set point. For multiple rotations it can be observed that this fluctuation is periodic and therefore likely caused by the installed Oldham couplings or manufacturing tolerances. On the other hand, the position step response shows a noticeable kink shortly before the set point is reached. Most likely, this is caused by static friction occurring when the velocity falls below a specific limit.

6. Summary and conclusion

Starting from a fundamental system model of the PMSM, a current-independent torque equation was derived and used to design a servo control setup that merely depends on encoder measurements. Experimental results have shown the performance of both the utilized speed estimator and the controller, which were implemented on an embedded system. However, although the cascaded controller is basically functional, there is still room for improvements.

Acknowledgements

This work is funded by the German Federal Ministry for Economic Affairs and Energy (BMWi), grant number KF2201091HM4, within the ZIM program.

References

- [1] J.C. Gamazo-Real, E. Vázquez-Sánchez, J. Gómez-Gil, Position and speed control of brushless DC motors using sensorless techniques and application trends, *Sensors* 10 (2010) 6901–6947.
- [2] P. Pillay, R. Krishnan, Modeling of permanent magnet motor drives, *IEEE Transactions on Industrial Electronics* 35, 4 (1988) 537–541.
- [3] B. Sahhary, *Elektr. Antriebe mit dauermagneterregten Maschinen im dyn. sensorlosen Betrieb*, Helmut-Schmidt-Universität, Hamburg (2008).
- [4] R. Petrella, M. Tursini, L. Peretti, M. Zigliotto, Speed measurement algorithms for low-resolution incremental encoder equipped drives: a comparative analysis, *IEEE International Aegean Conference on Electrical Machines and Power Electronics ACEMP'07 (2007)* 780–787.